Journal of Statistical Physics, Vol. 42, Nos. 3/4, 1986

Phonon Spectra in One-Dimensional Quasicrystals

J. M. Luck[1] **and D. Petritis**[2]

Received August 2, 1985

The propagation of phonons in one-dimensional quasicrystals is investigated. We use the projection method which has been recently proposed to generate almost periodic tilings of the line. We define a natural Laplace operator on these structures, which models phonon (and also tight-binding electron) propagation. The selfsimilarity properties of the spectrum are discussed, as well as some characteristic features of the eigenstates, which are neither extended nor localized. The long-wavelength limit is examined in more detail; it is argued that one is the lower critical dimension for this type of models.

KEY WORDS: Quasicrystals; quasiperiodic structures; Cantor spectrum; density of states; critical wave functions.

1. INTRODUCTION

The experimental discovery by Shechtman *et al.*[1] of a metallic solid phase of Al–Mn alloy with icosahedral symmetry has considerably revived interest in quasicrystals, since this point symmetry is inconsistent with conventional lattice translations. It was known from Penrose's work[2] that the plane can be tiled in a nonperiodic way by two types of rhombs. The crystallographic properties of these structures, and of generalizations of them in three dimensions, have been studied by several authors.[3,4]

More recently, different groups[5–8] have described an elegant and general way of generating a wide class of almost periodic tilings of euclidean p-dimensional space by projection from higher-dimensional regular lattices, either in direct (position) space or in reciprocal (momentum) space. Some of these structures have diffraction patterns which look identical to the experimental ones of Al–Mn alloys. The motivation in

[1] Service de Physique Théorique, CEN-Saclay, B.P. 2, 91191 Gif-sur-Yvette Cedex, France.
[2] CPT, Ecole Polytechnique, 91128 Palaiseaux Cedex, France.

0022-4715/86/0200-0289$05.00/0

studying physical properties of these quasicrystals is therefore twofold: they are realized in nature and possess an interesting mathematical structure.

The aim of this paper is to study the Laplace operator, which describes the propagation of harmonic vibrations (phonons) and of electrons (in the tight-binding approximation) on these structures. We shall restrict ourselves to the one-dimensional case, which already exhibits interesting features, in spite of its apparent simplicity. Our plan is the following: in Section 2, we describe some useful properties of the almost periodic chain obtained by the projection method from a square lattice; we define a one-parameter family of realistic Laplace operators and we discuss their possible applications. Section 3 is devoted to the spectrum of our model, with emphasis on its scaling properties and on the continuum (long wavelength) limit; we use in particular the renormalization group methods which have been applied to the similar problem of a discrete Schrödinger equation in a quasiperiodic potential. In Section 4, we discuss some particular features of the eigenfunctions; they are neither extended nor localized in the conventional sense. Some concluding remarks are presented in Section 5.

2. THE MODEL

The construction of a "one-dimensional quasicrystal," or almost periodic tiling of the line, by the projection method is explicitly given in Refs. 6 and 8. We reproduce it briefly. Consider in the Euclidean plane $\mathbb{R}^2$ the strip swept by shifting the unit square $(-1 < x \leqslant 0;\ -1 < y \leqslant 0)$ along the straight line $D(y = tx)$, where $t = \tan\theta$ and θ is the angle between D and the x axis. By projecting orthogonally onto D all points of the strip having integer coordinates, we get a sequence of points on D (see Fig. 1) which build the announced quasicrystal. A particularity of one-dimensional nonperiodic lattices is that they can always be viewed as a continuous deformation of the regular lattice $\mathbb{Z}$, since a sequence of points of the line has a natural ordering. Such an average regular lattice generally does not exist in dimension $p > 1$.

Let u_n denote the abscissa along D of the point number n, assuming that the label $n = 0$ is attached to the origin. The length $l_n = u_{n+1} - u_n$ of the bond joining points n and $n+1$ can only take the two values $s = \sin\theta$ or $c = \cos\theta$, corresponding, respectively, to projections of vertical or horizontal segments of the original lattice $\mathbb{Z}^2$. Let us associate with the right half of our chain an infinite word $w = scscc\ldots$, where each letter stands for the length $l_0, l_1, l_2, \ldots$ of the successive bonds. Whenever the slope $t = \tan\theta = p/q$ is a *rational* number, the tiling and the corresponding word w are *periodic*, with period $p+q$. When t is *irrational*, the tiling is a

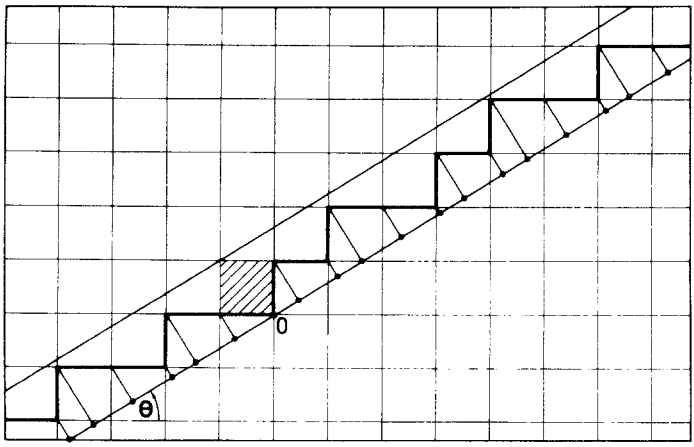

Fig. 1. Construction of a one-dimensional quasicrystal by the projection method.

quasicrystal. In more rigorous terms the sequence of bond lengths l_n is almost periodic.

Assume from now on that t is irrational and satisfies $0<t<1$. It is easy to realize that the letters s and c appear with frequencies $t/(t+1)$ and $1/(t+1)$ respectively in w, and hence that the average lattice spacing $\bar{l}$ reads

$$\bar{l}=\frac{t}{t+1}s+\frac{1}{t+1}c=\frac{1}{s+c} \tag{2.1}$$

A useful way of describing this type of quasiperiodic structure in one dimension is to introduce a so-called "hull function" g such that the abscissa of the nth point is given by

$$u_n=n\bar{l}+g(n) \tag{2.2}$$

One can easily deduce from the geometrical construction of Fig. 1 that the function g reads

$$g(x)=(c-s)\left[F\left(x\frac{t}{t+1}\right)-1\right] \tag{2.3}$$

where $F(y)$ denotes the fractional part of y, i.e., the difference between y and its integer part $[y]$.

Let us now give a complementary description of the word w, related to the continued fraction expansion of the slope t:

$$t=\cfrac{1}{r_1+\cfrac{1}{r_2+\cdots}}=[r_1, r_2,\ldots] \tag{2.4}$$

where $r_1 r_2,...$ are integers. By truncating this fraction at rank L, we obtain a rational number:

$$t_L = \frac{p_L}{q_L} = \cfrac{1}{r_1 + \cfrac{1}{r_2 + \cdots + \cfrac{1}{r_L}}} \tag{2.5}$$

called the Lth principal convergent of t. These numbers converge to t in such a way that

$$\frac{1}{2q_L q_{L+1}} < |t - t_L| < \frac{1}{q_L q_{L+1}} \tag{2.6}$$

The integers p_L and q_L obey the same recurrence relation:

$$\begin{aligned} p_L &= r_L p_{L-1} + p_{L-2} \\ q_L &= r_L q_{L-1} + q_{L-2} \end{aligned} \tag{2.7}$$

We have seen that the word w_L associated with the rational slope t_L is periodic; let W_L denote its unit cell: $w_L = W_L W_L W_L ...$; W_L contains $(p_L + q_L)$ letters. Let us show that W_L also obeys a three-terms recurrence relation, very reminiscent of (2.7), namely,

$$\begin{aligned} W_L &= W_{L-1}^{r_L} W_{L-2} \qquad (L \text{ even}) \\ W_L &= W_{L-2} W_{L-1}^{r_L} \qquad (L \text{ odd}) \end{aligned} \tag{2.8}$$

where multiplication is to be understood as word concatenation. The initial values of the recursion are: $W_0 = c$ (since $t_0 = 0$) and $W_1 = sc^{r_1}$ (since $t_1 = 1/r_1$). It is easy to check that Eq. (2.8) indeed gives the correct number of letters s and c in the cell W_L. We shall prove that the *ordering* imposed by (2.8) is the right one.

To do so, consider the geometrical construction of the cell W_L corresponding to the rational slope t_L. Starting from the origin, we move to the nearest neighbor of $\mathbb{Z}^2$ lying in the strip: $t_L x \leqslant y < t_L x + t_L + 1$, and repeat the procedure according to

$$(\mu; \nu) \to \begin{cases} (\mu; \nu + 1) & \text{if} \quad \mu/(\nu + 1) \geqslant t_L \text{ (letter } c) \\ (\mu + 1; \nu) & \text{if} \quad \mu/(\nu + 1) < t_L \text{ (letter } s) \end{cases} \tag{2.9}$$

since letters c and s denote horizontal and vertical motions, respectively. The procedure is ended if $(\mu; \nu)$ lies on the line D; this happens first for $(\mu; \nu) = (q_L, p_L)$. The crucial point in the derivation of (2.8) lies in the

fact that t_L converge alternatively to t: the even subsequence is strictly increasing and the odd one strictly decreasing:

$$t_{2l-2} < t_{2l} < \cdots < t < \cdots < t_{2l+1} < t_{2l-1} \tag{2.10}$$

Assume from now on that $L = 2l$ is even (the case of odd L is treated in an analogous way). Let $\mu < p_{2l}$ and $\nu < q_{2l}$ be the coordinates of a point of the strip, such that its next horizontal neighbor lies outside the strip, i.e., $\mu/(\nu+1) \leqslant t_{2l} < \mu/\nu$. Using the fact that $t_0, \ldots, t_{2l-2}$, t_{2l-1} are also principal convergents of t_{2l}, we show that

$$\mu/(\nu+1) \leqslant t_{2l} < t_{2l-1} \leqslant \mu/\nu \tag{2.11}$$

Therefore vertical moves concide for these points for slopes t_{2l} and t_{2l-1}. Next, we show that (2.8) gives the only possible ordering. This is readily done by using the following inequality:

$$r_{2l} q_{2l-1} t_{2l} \leqslant r_{2l} p_{2l-1} \leqslant r_{2l} q_{2l-1} t_{2l} + t_{2l} + 1 \tag{2.12}$$

which is itself a simple consequence of classical inequalities on the principal convergents.

Let us now define a Laplace operator Δ acting on scalar quantities φ_n according to

$$(\Delta\varphi)_n = \frac{\varphi_{n+1} - \varphi_n}{\lambda_n} - \frac{\varphi_n - \varphi_{n-1}}{\lambda_{n-1}} \tag{2.13}$$

where the λ_n are couplings attached to the lattice bonds. We assume that λ_n only depends on the length l_n, i.e., λ_n has two possible values, say, $\lambda_n = \lambda_s$ for short bonds ($l_n = s$), and $\lambda_n = \lambda_c$ for long bonds ($l_n = c$). It is reasonable to choose $\lambda_s < \lambda_c$, implying that neighboring sites are more strongly coupled if the distance between them is smaller. In the following, we choose units such that $\lambda_c = 1$, and keep $\lambda_s = \rho < 1$ as a free parameter. It has been pointed out[9] that there is a special choice of the couplings λ_n, namely, λ_n proportional to the lengths l_n, such that Δ acting on linear functions $\varphi_n = A + Bu_n$ of the coordinate u gives identically zero, just as the differential operator d^2/du^2. In the present model, this special Laplacian corresponds to the value $\rho = t$. We shall see hereafter that this value is not singled out in the physical properties of our model, and that the essential features of the operator Δ are qualitatively independent of the value of ρ.

The eigenfunctions φ and associated eigenvalues $z > 0$ of the operator $(-\Delta)$ satisfy

$$\frac{\varphi_{n+1} - \varphi_n}{\lambda_n} - \frac{\varphi_n - \varphi_{n-1}}{\lambda_{n-1}} + z\varphi_n = 0 \tag{2.14}$$

This equation appears in a natural way in several physical problems. The study of harmonic vibrations of the quasicrystal (phonon spectrum) leads to an equation of the form (2.14), where φ_n is the displacement of the nth atom, λ_n the elastic coupling (inverse spring constant) between atoms n and $n+1$, and z denotes the squared eigenfrequency ω^2 in reduced units. Note that in higher dimension the displacement of an atom is a vector, and hence the eigenmode equation for phonons is more complicated than the scalar equation (2.14). The Schrödinger equation for electrons in the tight-binding approximation also leads to equation (2.14) if the site potentials V_n are equal to a constant V, and if λ_n are the hopping matrix elements between neighboring sites; φ_n is now the amplitude of the wave function at site n, and z is proportional to $(E-V)$ where E is the energy of the state. More generally, any kind of propagation or diffusion problems for which all sites are equivalent, and only the nature of the bonds matters, can be modelized by equations involving a discrete Laplacian of the type (2.13).

3. PROPERTIES OF THE SPECTRUM

In order to study the spectrum of our Laplacian, it is convenient to introduce variables Q_n which live on the *bonds* of the quasicrystal, and hence are dual to the φ_n. The two types of variables are related through

$$Q_n = (\varphi_{n+1} - \varphi_n)/\lambda_n \tag{3.1a}$$

$$\varphi_n = (Q_{n-1} - Q_n)/z \tag{3.1b}$$

and the eigenfunction equation (2.14) becomes in terms of the Q_n:

$$Q_{n+1} - 2Q_n + Q_{n-1} + z\lambda_n Q_n = 0 \tag{3.2}$$

Equation (3.2) expresses that Q_n is an eigenfunction associated with *eigenvalue* 0 for the operator $H = -\Delta_0 + V$, where Δ_0 is the usual discrete Laplacian on a regular lattice, and the potentials $V_n = -z\lambda_n$. The transformation $\varphi \to Q$ has been introduced by Gardner *et al.*,[10] who study the operator Δ on a random chain.

The rigorous study of Schrödinger equations with almost periodic potentials has recently produced numerous mathematical results (see Ref. 11 for a review). The present problem amounts to finding the values of the potential strength z such that the operator H has a zero eigenvalue, while one is usually interested in finding the eigenvalues for a fixed potential. Although the problems are *a priori* different, they have a large number of common features.

A convenient way of dealing with Eq. (3.2) is to introduce the transfer matrix formalism. Equation (3.2) can be recast in the following matrix form:

$$\begin{pmatrix} Q_{n+1} \\ Q_n \end{pmatrix} = T_n \begin{pmatrix} Q_n \\ Q_{n-1} \end{pmatrix} \qquad \text{with } T_n = \begin{pmatrix} 2 - z\lambda_n & -1 \\ 1 & 0 \end{pmatrix} \tag{3.3}$$

where λ_n assumes the value ρ or 1, according to the value of the nth letter in the word w. Equation (3.3) is easily iterated and yields

$$\begin{pmatrix} Q_n \\ Q_{n-1} \end{pmatrix} = T_{n-1} T_{n-2} \cdots T_1 \begin{pmatrix} Q_1 \\ Q_0 \end{pmatrix} \tag{3.4}$$

This elegant version of Eq. (3.2) is of course particular to one-dimensional models. Another remarkable property in one dimension is the fact that the integrated density of states (IDS) $H(z)$, defined as being the fraction of eigenvalues which are less than z, is also equal to the asymptotic number of times the solution Q of Eq. (3.2) changes its sign per unit length. This also holds for values of z which are not in the spectrum. In the case of continuous Schrödinger equations, where $H = -d^2/dx^2 + V(x)$, the quantity $\kappa(z) = H(z)/2$ is the average number of times the phase of the wave function rotates per unit length, and is often called rotation number at energy z.

The case of a rational slope $t = p/q$ is very well understood. We have seen that the word w is periodic, with period $p+q$. The eigenfunctions of our Laplacian obey Bloch theorem, and the spectrum generally consists of $(p+q)$ bands; in each band, the eigenfunction Q is a Bloch wave labeled by a wave vector k such that $\mathrm{tr}(T_{p+q} \cdots T_1) = 2 \cos k$. In the gap between bands having number m and $(m+1)$, the IDS has the constant value $H(z) = m/(p+q)$.

Let us return to the case of an irrational slope t. We shall treat in great detail the example of the inverse golden mean: $t = \sigma^{-1} = \sigma - 1$ with $\sigma = (\sqrt{5}+1)/2$, keeping in mind that the specific results we obtain for this special value are generalizable to values of t which have the most typical diophantine properties, i.e., are not too well approximated by rationals.[9] The inverse golden mean contains only the number 1 in its continued fraction expansion ($r_1 = r_2 \cdots = 1$); it is hence the number which is the worst approximated by rationals, and also the number for which the lack of periodicity of our quasicrystal is expected to have quantitatively the most spectacular consequences.

The rational approximants t_L of t defined in Section 2 are $t_L = F_L/F_{L+1}$, where F_L are the Fibonacci numbers, defined by $F_0 = 0$,

$F_1 = 1$, and the recursion relation $F_L = F_{L-1} + F_{L-2}$. The associated cells W_L of the periodic words w_L therefore satisfy

$$\begin{aligned} W_0 &= c & W_1 &= sc \\ W_L &= W_{L-1} W_{L-2} & (L \text{ even}) & \\ W_L &= W_{L-2} W_{L-1} & (L \text{ odd}) & \end{aligned} \tag{3.5}$$

Note that W_L has length F_{L+2}. The corresponding transfer matrices $\tau_L = T_{F_{L+2}-1} \cdots T_2 T_1$ obviously obey the same recursion relations (with the opposite order of factors, since matrix products are read from right to left). It can then be shown[12] that the quantities

$$x_L = \frac{1}{2} \operatorname{tr} \tau_L \tag{3.6}$$

obey the following four-terms recursion relation:

$$x_L = 2x_{L-1} x_{L-2} - x_{L-3} \tag{3.7}$$

while a convenient way to put the initial conditions is

$$x_{-2} = 1, \qquad x_{-1} = 1 - \rho z/2, \qquad x_0 = 1 - z/2$$

The remarkable relation (3.7) has been the starting point of a renormalization group treatment of almost periodic potential models involving the golden mean.[12-16] In the present model, it is a simple consequence of Eq. (3.5), which holds for arbitrary values of ρ and z. It will allow us to understand quantitatively the scaling properties of the spectrum, in analogy with the work of Kohmoto *et al.*[12-14] and of Ostlund *et al.*[15,16]

The IDS $H(z)$, computed from the number of changes in the sign of Q_n as explained above, is plotted on Fig. 2, for $\rho = 0.5$. Its most characteristic point, namely, the presence of gaps at all length scales, is present for all values of $\rho < 1$. It is indeed a generic feature of almost periodic Laplace operators that their spectrum is a Cantor set. The dashed curve represents the IDS of the underlying average lattice [where all λ_n have been replaced by their average $\bar{\lambda} = (t\rho + 1)/(t + 1)$]:

$$H_{av}(z) = \frac{1}{\pi} \cos^{-1}\left(1 - \frac{z\bar{\lambda}}{2}\right) \tag{3.8}$$

The difference between both curves is hardly visible for small energies ($z < 1$); we shall return to that limit at the end of the section.

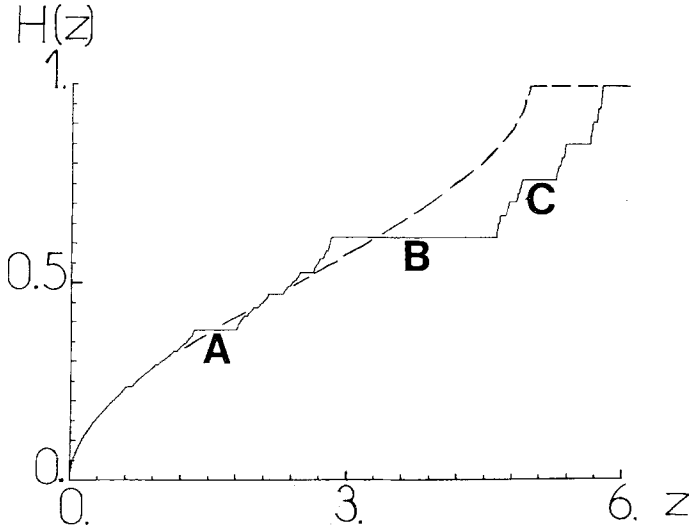

Fig. 2. Plot of the integrated density of states $H(z)$ of the quasicrystal with $t=\sigma^{-1}$ and $\rho=0.5$ (full curve), and of the underlying average lattice (dashed curve).

In the above-mentioned discontinuous almost periodic potential models, the authors of Refs. 12–14 have related scaling properties of the spectrum to the presence of a particular six-cycle in the trace mapping (3.7): $a\to 0\to 0\to -a\to 0\to 0$, where a depends continuously on the potential strength. In the present case, we have realized from *numerical* data that the self-similarity properties of the spectrum were governed by *another* six-cycle of the same mapping, namely, $\alpha\to -\beta\to -\alpha\to \beta\to -\alpha\to -\beta$, where the positive numbers α and β are the following functions of ρ and z:

$$\alpha,\beta = X\pm (X^2-X)^{1/2} \qquad \text{with} \quad X=\tfrac{1}{8}\{3+[25+4(1-\rho)^2 z^2]^{1/2}\} \tag{3.9}$$

Our argument will closely follow that of Ref. 14. Let $\Lambda(z)$ denote the largest eigenvalue of the mapping obtained by linearizing the trace mapping (3.7) around the six-cycle we have just described. Then a small part of the spectrum around some energy z will reproduce itself up to a dilation factor $\Lambda(z)$ when the approximant t_L is replaced by t_{L+6}. We claim that this scaling behavior remains valid in the infinite system at the upper bound $z_{\max}$ of the spectrum, and more generally at each *gap edge*. Let us take the example of the upper bound for simplicity. Let z_L denote the lower bound of the last band corresponding to the approximant t_L: $1-H(z_L)=1/F_{L+2}$. When L is replaced by $L+6$, then $(z_{\max}-z_L)$ is

asymptotically divided by $\Lambda(z_{\max})$, while $1-H(z_{L+6})=1/F_{L+8}\sim \sigma^{-6}/F_{L+2}$. It can be argued from this analysis that $H(z)$ exhibits the following power-law behavior in the vicinity of $z_{\max}$:

$$1-H(z)\sim(z_{\max}-z)^{\Delta}\,P[\ln(z-z_{\max})] \tag{3.10}$$

where the exponent Δ stands for $\Delta(z_{\max})$ with

$$\Delta(z)=\frac{6\ln\sigma}{\ln\Lambda(z)} \tag{3.11}$$

and P is a periodic amplitude with period $\ln\Lambda$. Figure 3 shows a log–log plot of $1-H(z)$ against $z_{\max}-z$, for $\rho=0.5$. The straight line has the theoretical slope $\Delta=0.427174$. The observed period (one period between gaps D and F, etc.) is actually three times smaller than the prediction $\ln\Lambda=6.758998$; in other words, the scaling of $H(z)$ is as if the six-cycle were a two-cycle $\alpha\to\beta$, forgetting about the signs.

In each gap, the IDS takes a (constant) value which is a linear combination, with integer coefficients, of the two incommensurate frequencies appearing in the couplings λ_n, i.e., 1 and $t/(1+t)$, or equivalently 1 and σ in our case. This property is the well-known "gap labeling theorem" (see

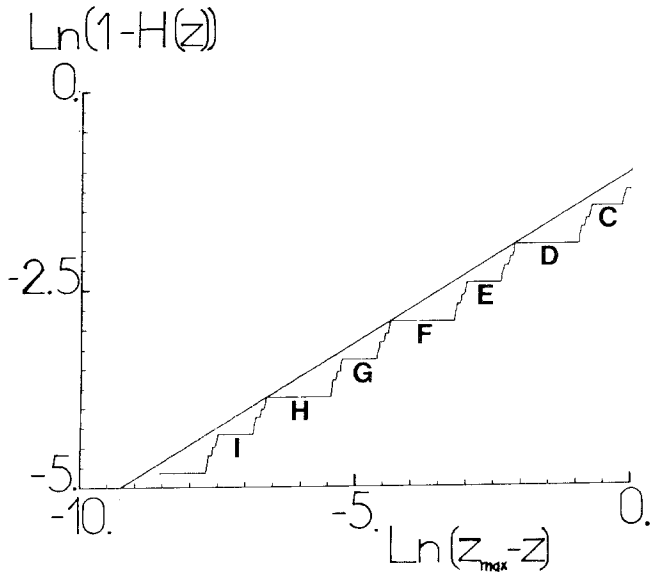

Fig. 3. Log–log plot of $1-H(z)$ against $z_{\max}-z$, for $\rho=0.5$, showing the scaling behavior of the spectrum at its upper bound. The straight line has the theoretical slope $\Delta=0.427174$.

Ref. 9 and references therein). The letters A, B, C,... on Figs. 2 and 3 show a particular sequence of gaps, which contains the largest ones, where the labeling of the IDS involves two adjacent Fibonacci numbers:

$$H_k = 1 + (-1)^k(\sigma F_k - F_{k+1}) = 1 - \sigma^{-k} \tag{3.12}$$

A, B, C,... correspond to $k = 1, 2, 3,...$, respectively. The presence of two of these gaps per asymptotic period $(\ln A)/3$ in $\ln(z_{\max} - z)$ is of course consistent with Eq. (3.11). The power-law behavior (3.11) is present around each gap edge z such that the associated sequence $x_n(z)$ is attracted by the six-cycle we have singled out. Our numerical experience leads us to conjecture that this indeed happens for *all* gap edges, i.e., on a set which is denumerable but dense in the spectrum. A very similar dense set of power-law singularities modulated by log-periodic amplitudes has been recently described[17] in the IDS of a random one-dimensional harmonic alloy model.

We end our study of the spectrum by looking at the small-frequency limit ($z \to 0$). We have seen in Fig. 2 that the IDS $H(z)$ approaches the value $H_{av}(z)$ corresponding to the underlying average (periodic) lattice very rapidly as $z \to 0$. In particular, gaps are hardly visible for $z < 0.6$. Although $H(z)$ looks very smooth in this region, we now argue that the spectrum has no absolutely continuous component. In other words, for almost all values of z, the x_n of the trace mapping (3.7) escape at infinity. In order to get a numerical evidence of this claim, as well as a more quantitative understanding of the long wavelength limit, we have computed the *mean escape time* $T(z)$ of the trace mapping in the following way. Let $N(z)$ be the smallest integer such that $|x_n| > 10^{10}$, where x_n are the iterates of the trace mapping. Note that $N(z)$ is not defined at points, such as the gap edges, which lead to bounded orbits. Define $T(z)$ as being the average of $N(z')$ over a small interval around z: $z(1-\delta) < z' < z(1+\delta)$. We observe from the numerical data the following facts: $T(z)$ is a well-defined quantity for all values of z; it is in particular independent of the width δ for small enough δ. Moreover, it is a very regular function of z, which very clearly behaves as

$$T(z) \sim \frac{C(\rho)}{z} \tag{3.13}$$

as z goes to zero, and the coefficient $C(\rho)$ is itself a very smooth function of ρ, which we have plotted on Fig. 4. It is obvious that, if we had chosen another large number instead of 10^{10} to decide when x_n escapes to infinity, this would have changed $N(z)$ and $T(z)$ by a *finite* amount, and hence left

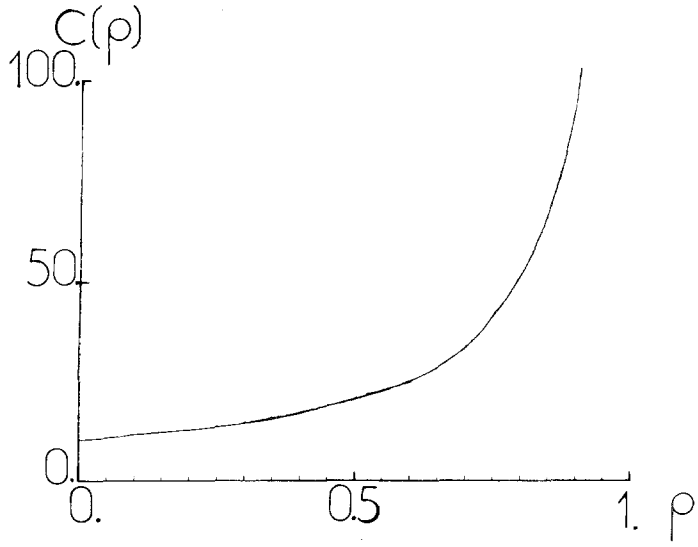

Fig. 4. Plot of the amplitude $C(\rho)$ of the small z behavior of the mean escape time $T(z)$ [see Eq. (3.13)].

unchanged $C(\rho)$, which has a physical meaning, as will be discussed at the end of next section.

We have also computed the total bandwidth B_L of the spectrum corresponding to the rational approximants t_L. In the models with a discontinuous quasiperiodic potential, the total bandwidth decreases as $B_L \sim F_L^{-\delta}$, i.e., $B_L \sim \sigma^{-L\delta}$,[12-16] where δ is some exponent related to the potential strength. In the present model, this exponential decrease of the total bandwidth as a function of the order L of the approximant is absent, because of the small-z region, where the widths of the first few *bands* scale as σ^{-2L} [since $\Delta(0) = \sigma^{12}$], while the widths of the first few *gaps* scale as σ^{-4L}. This phenomenon occurs for values of z such that $L \lesssim T(z)$. The contribution of this region to B_L therefore scales as L^{-1}. Since gaps and bands have comparable widths outside this region, we expect that the total bandwidth also behaves as

$$B_L \sim \kappa(\rho)\, L^{-1} \tag{3.14}$$

Figure 5 shows a log–log plot of the reduced bandwidth $B_L/z_{\max}$ against L for different values of ρ. The straight dashed line has slope -1. The numerical data are compatible with the conjecture (3.14). In any case, B_L clearly goes to zero as L goes to infinity. We would like to deduce from this fact a more rigorous argument in favor of the absence of an absolutely continuous component in the spectrum in the quasiperiodic case. To do so, we

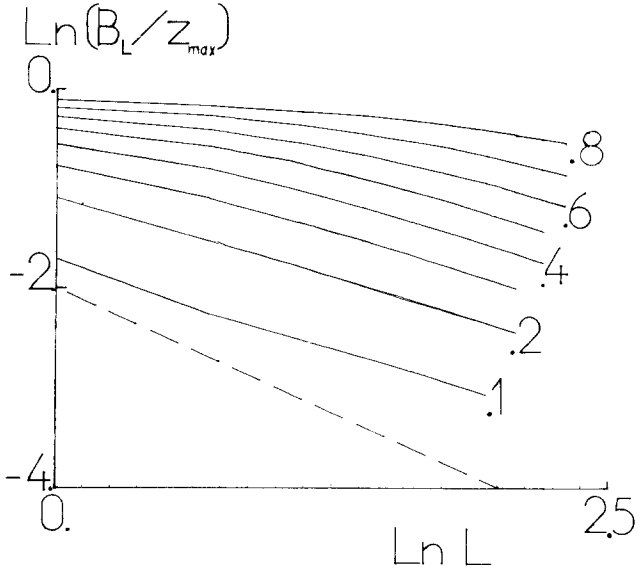

Fig. 5. Log–log plot of the reduced bandwidth $B_L/z_{\max}$ against the order L of the rational approximant to the golden mean. The numbers indicate the values of the parameter ρ. The dashed line has slope -1.

have to consider a slightly more general model, and allow for a phase in the hull function describing the abscissas u_n. This amounts to translating the strip to an arbitrary position in the plane $\mathbb{R}^2$, instead of demanding that the line D passes through the origin. Consider the sequence of points given by

$$u_n = n\bar{l} + g(n+\alpha) \tag{3.15}$$

where $\bar{l}$ and g are as in Section 2, and α is an arbitrary phase. Assume that $t = \tan\theta = p/q$ is rational: the sequence of bond lengths $l_n = u_{n+1} - u_n$ is then periodic, with period $p+q$. A remarkable property of this sequence is that it is *independent* of the phase α, up to a translation on the label n. It is indeed very easy to realize that this sequence remains unchanged when α describes the interval $0 \leqslant \alpha < 1/(p+q)$, and it can be shown that there always exists some n_0 such that the translation $n \to n - n_0$ is equivalent to the change of α into $\alpha - [(p+q)\alpha]/(p+q) = \alpha'$ which indeed satisfies $0 \leqslant \alpha' < 1/(p+q)$. The spectrum of the Laplacian in the rational cases is therefore independent of the phase α, i.e., invariant under translation of the strip in the plane. This is sufficient to conclude that the Lebesgue measure of the spectrum corresponding to $t = \sigma^{-1}$ is equal to $\lim_{L\to\infty} B_L$, i.e., vanishes.

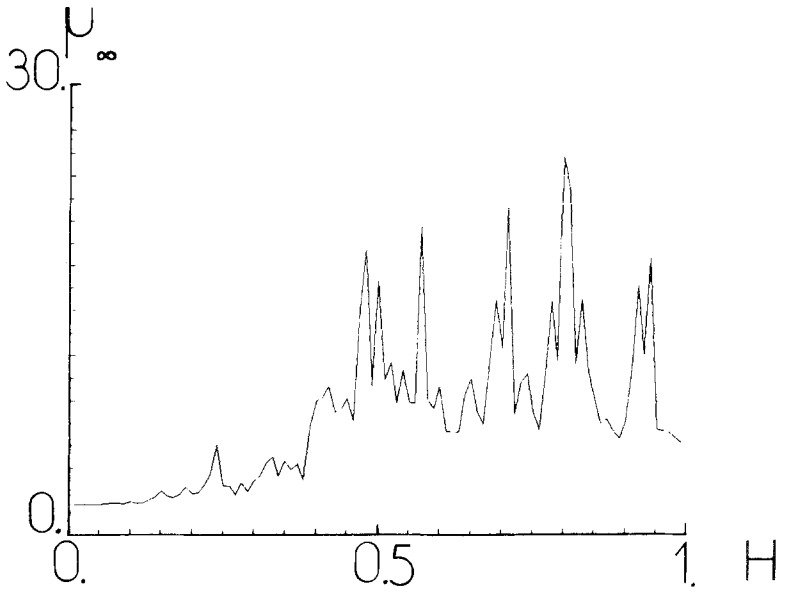

(a)

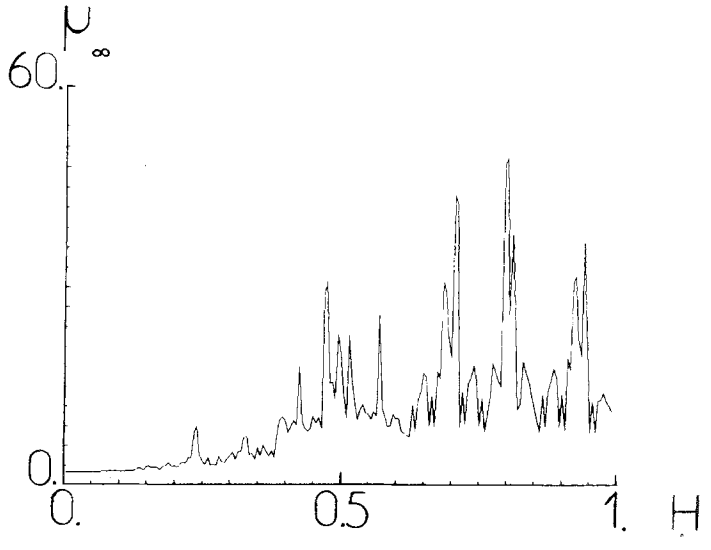

(b)

Fig. 6. Plot of the moment μ_∞ defined in Eq. (4.2) for all eigenstates of a system of size N with $\rho = 0.5$. (a) $N = 100$, (b) $N = 200$, (c) $N = 400$, (d) $N = 800$.

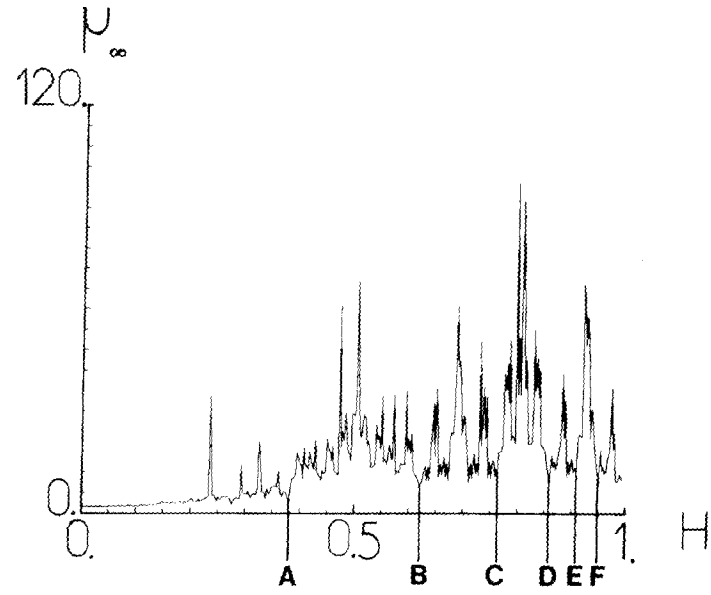

(c)

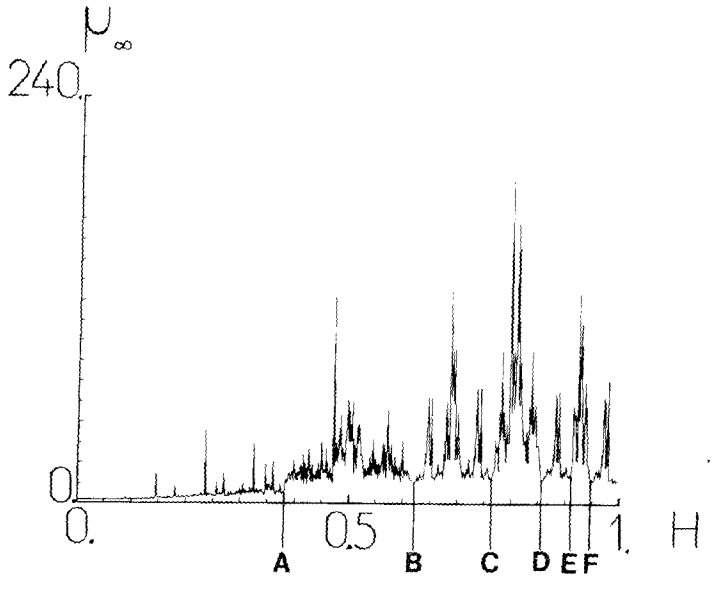

(d)

Fig. 6 (*continued*)

4. PROPERTIES OF THE EIGENSTATES

We now turn to the more difficult problem of characterizing the eigenstates of our Laplace operator. We already know that our model has no absolutely continuous spectrum, and hence no conventional extended (Bloch) states. We claim that it also has no localized (normalizable) eigenstates: although we have no proof of this statement in the case of the golden mean, and even no clear cut numerical evidence, it has been proven by Delyon and Petritis[18] that there exists no normalizable eigenstate for Schrödinger equations with a discontinuous almost periodic potential if the irrational slope t contains in its continued fraction expansion an infinity of integers r_L obeying $r_L \geqslant 5$. Although the golden mean does not belong to that class, almost all irrationals having typical diophantine properties do belong to it. We find it therefore reasonable to conjecture that our Laplace operator has only singular continuous spectrum and only "critical" eigenstates for *all* typical irrational values of t. This conjecture was in fact already formulated by Kohmoto[14] for the Schrödinger equation in a discontinuous quasiperiodic potential.

In order to characterize these "critical" states more precisely, we have computed numerically all the eigenstates of our Laplacian on a sample of

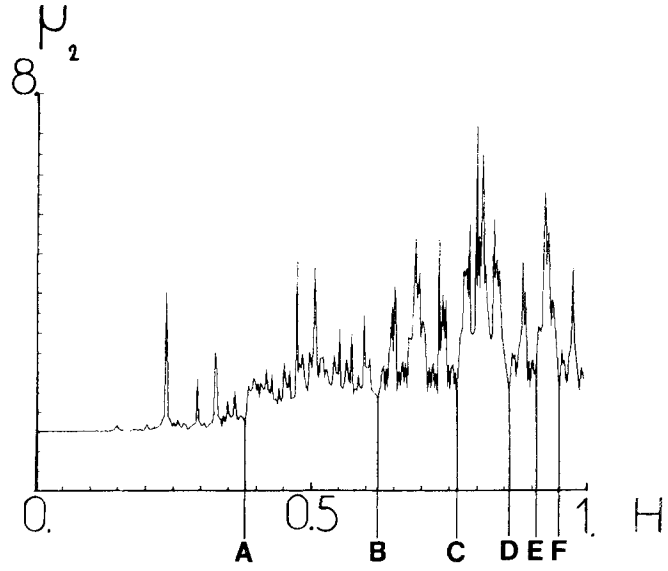

Fig. 7. Plot of the moment μ_2, related to the IPR, defined in Eq. (4.1), for a system size $N = 400$ and $\rho = 0.5$.

large but finite size (number of sites) N, with Dirichlet boundary conditions ($\varphi_0 = \varphi_{N+1} = 0$). There are N such states, which are conveniently labeled by k, number of times φ changes its sign ($1 \leqslant k \leqslant N$). For large N, the kth state has an energy z such that $H(z) \approx k/N$.

Let us define for each eigenstate φ the following reduced moments:

$$\mu_l = \left(\frac{1}{N} \sum_{n=1}^{N} \varphi_n^{2l} \right)^{1/l} \tag{4.1}$$

The first moment μ_1 is just the usual squared L^2 norm: all the states are assumed to be *normalized* such that $\mu_1 = 1$ in the following. The moment μ_2 is related to the inverse participation ratio (IPR), commonly used in numerical work on localization, through: $\mu_2^2 = N$. IPR. As l goes to infinity, the μ_l have a well-defined limit:

$$\mu_\infty = \operatorname*{Sup}_{1 \leqslant n \leqslant N} \varphi_n^2 \tag{4.2}$$

which is just the squared L^∞ norm of the state. A simple way of looking at the "shape" of the eigenstate φ is to examine the behavior of the moments $\mu_l(N)$ for large N. It is clear that $\mu_l(N)$ admit *finite* limits as $N \to \infty$ for

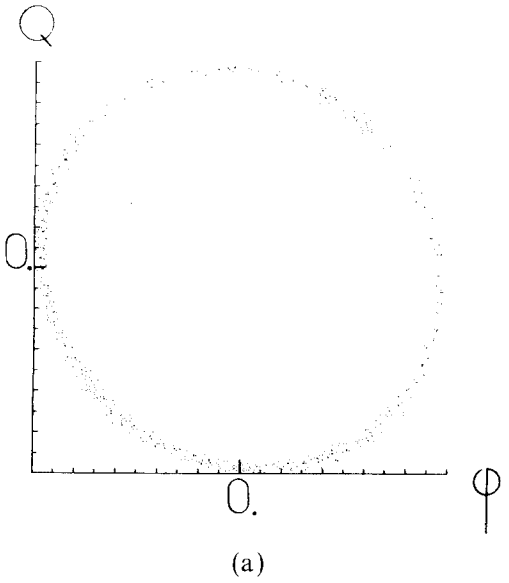

(a)

Fig. 8. Phase portraits in the (φ, Q) plane of some typical eigenstates of a system with $N = 1000$ sites and $\rho = 0.5$. The IDS of the states read (a) 61/1000, (b) 262/1000, (c) 528/100, (d) 620/1000, (e) 933/1000. The units on the axes are such that Sup $|\varphi| =$ Sup $|Q| = 1$.

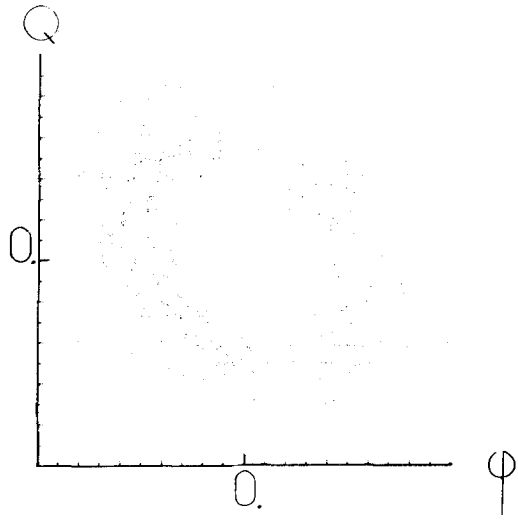

(b)

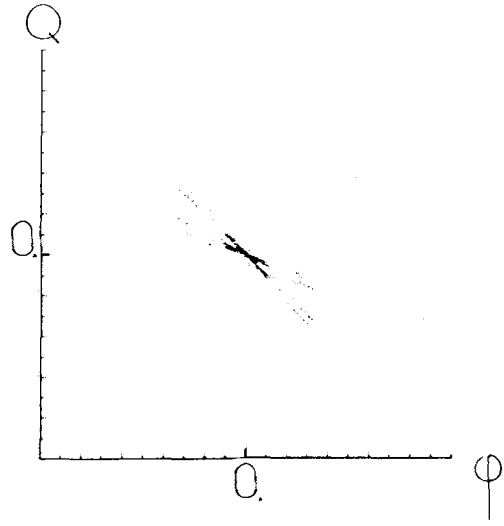

(c)

Fig. 8 (*continued*)

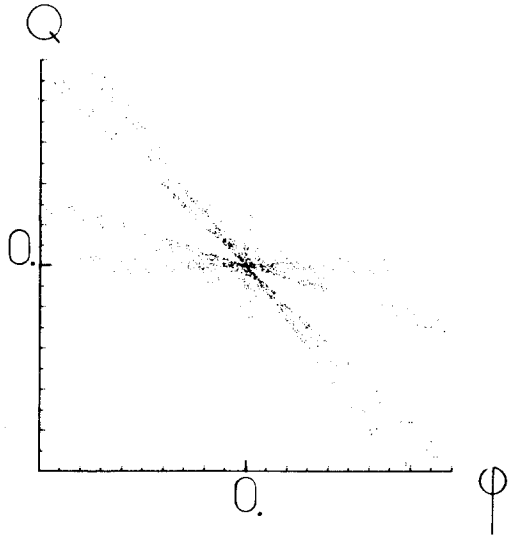

(d)

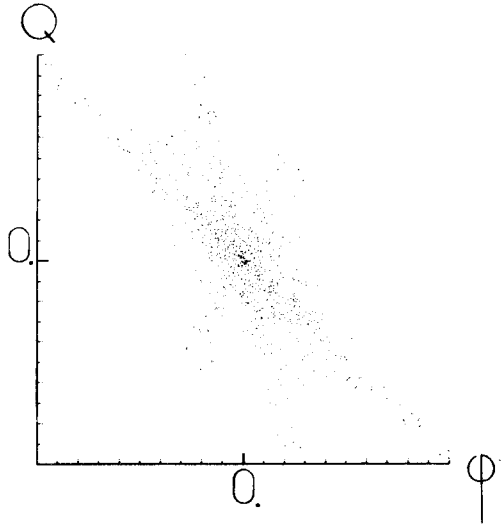

(e)

Fig. 8 (*continued*)

states which "will be" conventionally extended on the infinite chain, while $\mu_l(N) \sim N^{1-1/l}$ for localized (normalizable) states.

Figure 6 shows plots of the moment μ_∞ for all eigenstates of our Laplacian for $t = \sigma^{-1}$, $\rho = 0.5$, and (a) $N = 100$, (b) $N = 200$, (c) $N = 400$, (d) $N = 800$. The abscissas are the values of the IDS ($H = k/N$ for the kth state). For the first few levels ($H \to 0$ or $z \to 0$) μ_∞ goes to the value 2, which is precisely the value of μ_∞ for the eigenstates $\varphi_n = \sin(nk\pi/N)$ on a regular lattice. We shall return to that point later on.

These plots exhibit peaked structure down to the smallest possible scale $\delta H = 1/N$: neighboring states have very contrasted "shapes," even for large system sizes. The plots corresponding to the largest two sizes, in Figs. 6c and 6d, show very interesting self-similarity properties, in close relationship with those of the IDS we have discussed in Section 3. In particular, the main sequence of gaps, labeled A, B, C,... in the last section, are clearly visible as deep local minima of $\mu_\infty(H)$. The intervals between these gaps show a three-fold structure (see between B–C, C–D, D–E, etc. as well as between B and the upper bound, between D and the upper bound, etc.). The IDS (see Fig. 3) shows a fully similar three-fold structure at the very same places. Figure 7 shows a plot of the moment μ_2 for the same values of t and ρ, and a sample length $N = 400$. The $H \to 0$ limit of μ_2 is again in agreement with the value $(3/2)^{1/2}$ corresponding to plane waves on a regular lattice. Figures 6c and 7 show that the quantities μ_∞ and μ_2 exhibit identical self-similarity properties.

We can deduce from these plots the following rough empirical rule: the farther a state is from large gaps in the spectrum, the larger its moments μ_l are (at fixed size N), i.e., the more it looks like a localized state. We have unfortunately not succeeded in putting this experimental evidence in a more quantitative way.

We discuss now a totally different way of looking at the eigenstates of our Laplace operator. Equation (3.1) suggests that the quantities φ_n and Q_n are very analogous to coordinate x and momentum p of a classical harmonic oscillator, obeying $\dot{x} = p$ and $\dot{p} = -\omega^2 x$. We therefore propose to look at the eigenstates in their phase space (φ, Q). If we solve equation (2.14) on a system with N sites, then each eigenstate is represented by a set of N discrete points in that (φ, Q) plane. On a regular lattice, the plane wave $\varphi_n = \sin(nk\pi/N)$ gives rise to points which become dense on an *ellipse* as N gets large, while a localized state gives a small dark spot at the origin, plus a few points away, corresponding to the few sites where the wave function is appreciably different from zero. Figure 8 shows some typical "phase portraits" we have obtained for $N = 1000$ and $\rho = 0.5$. The states are again identified by their IDS: (a) 61/1000, (b) 262/1000, (c) 528/1000, (d) 620/1000, (e) 933/1000. The units on the axes are such that

Sup $|\varphi| = \text{Sup } |Q| = 1$. As the IDS increases from zero to unity, the image turns smoothly from a loose ellipse (a) to a star (e) radiating from the origin with an intricate angular structure. The crossover between the two regimes occurs at the value of z for which the system size N is of the order of magnitude of the following length:

$$\xi(z) = \sigma^{T(z)} \sim e^{[C(\rho) \ln \sigma]/z} \tag{4.3}$$

which is the length scale associated with the mean escape time discussed in Section 3. For $N \ll \xi$, the wave functions do not feel the lack of periodicity of the quasicrystal, and *roughly* behave as Bloch states (note nevertheless the dispersion over a finite width of the points around the average ellipse in Fig. 8a). For $N \gg \xi$, the states are in the critical regime. There is in particular a large probability for φ_n and Q_n to be simultaneously small, but the regions where φ is large are not spatially localized. The characteristic length scale $\xi(z)$ is not a localization length (since our eigenstates are not localized), but rather a "memory" length, beyond which the wave function loses memory of its initial phase. It is quite remarkable that ξ diverges exponentially as $z \to 0$, while the localization length of *random* systems of the same type only diverges as $\xi_{\text{loc}} \sim 1/z$.

5. CONCLUSIONS

The present work shows that phonon propagation in quasicrystals already has quite interesting features in the very particular case of one dimension.

The generic properties of typical irrationals have been studied in the example of the golden mean. As far as the spectrum is concerned, its scaling properties are explained by the trace mapping (3.7), which has already been used in the context of quasiperiodic potentials. This self-similarity implies that the IDS exhibits singular power-law behavior (3.10) at a dense set of points; this property is reminiscent of a recent work[17] on the spectrum of a similar Laplace operator on a random chain, where the masses (analogous to our couplings λ_n) can only assume two values.

The difficult question of characterizing the states has been partly answered. We have now strong evidence that the eigenstates are neither extended nor localized in the usual sense. Let us emphasize that the fact that *all* states are critical for arbitrary values of ρ and all typical irrational values of t, although already conjectured by Kohmoto *et al.*, is still a non-intuitive and surprising result. Besides the interesting self-similar structures showing up in the plots of the moments μ_l, and in the phase portraits of

the eigenstates, the most remarkable quantitative feature seems to be the exponential divergence of the "memory length" $\xi(z)$ at small energy.

This type of essential singularity is also present in the localization length in *two*-dimensional random potential models, and more generally in every simple statistical mechanical model at its marginal (lower critical) dimensionality. We are therefore tempted to expect that the marginal dimension of the Laplacian on quasicrystals is *one*, and hence that absolutely continuous spectrum and extended quasi-Bloch-type states will occur for low enough energy in two and higher dimensions. We hope to return to that subject in a future publication.

ACKNOWLEDGMENTS

It is a pleasure to thank S. Aubry, J. Bellissard, F. Delyon, C. Godrèche, P. Moussa, and F. Vallet for useful comments, and especially C. Itzykson for discussions which motivated the present work.

REFERENCES

1. D. Shechtman, I. Blech, D. Gratias, and J. W. Cahn, *Phys. Rev. Lett.* **53**:1951 (1984).
2. R. Penrose, *Bull. Inst. Math. Appl.* **10**:266 (1974); *Math. Intell.* **2**:32 (1979); M. Gardner, *Sci. Am.* **236**:110 (1977).
3. A. L. Mackay, *Sov. Phys. Cryst.* **26**:517 (1981).
4. D. Levine and P. J. Steinhardt, *Phys. Rev. Lett.* **53**:2477 (1984).
5. P. Kramer and R. Neri, *Acta Cryst.* **A40**:580 (1984).
6. R. K. P. Zia and W. J. Dallas, *J. Phys.* **A18**:L341 (1985).
7. M. Duneau and A. Katz, *Phys. Rev. Lett.* **54**:2688 (1985).
8. V. Elser, *Phys. Rev.* **B32**:4892 (1985).
9. N. H. Christ, R. Friedberg, and T. D. Lee, *Nucl. Phys.* **B202**:89 (1982); **B210**:310, 337 (1982); C. Itzykson, in Progress in Gauge Field Theory, Proceedings of the Cargèse summer school 1983, edited by G. 't Hooft *et al.*
10. E. J. Gardner, C. Itzykson, and B. Derrida, *J. Phys.* **A17**:1093 (1984).
11. B. Simon, *Adv. Appl. Math.* **3**:463 (1982).
12. M. Kohmoto, L. P. Kadanoff, and C. Tang, *Phys. Rev. Lett.* **50**:1870 (1983).
13. M. Kohmoto, *Phys. Rev. Lett.* **51**:1198 (1983).
14. M. Kohmoto and Y. Oono, *Phys. Lett.* **102A**:145 (1984).
15. S. Ostlund, R. Pandit, D. Rand, H. J. Schellnhuber, and E. D. Siggia, *Phys. Rev. Lett.* **50**:1873 (1983).
16. S. Ostlund and R. Pandit, *Phys. Rev. B* **29**:1394 (1984).
17. Th. M. Nieuwenhuizen and J. M. Luck, *J. Stat. Phys.* **41**:745 (1985).
18. F. Delyon and D. Petritis, *Comm. Math. Phys.* (to appear).